Oocytes can efficiently repair DNA double-strand breaks to restore genetic integrity and protect offspring health

Jessica M. Stringer[a,b], Amy Winship[a,b], Nadeen Zerafa[a,b], Matthew Wakefield[c,d], and Karla Hutt[a,b,1]

[a]Ovarian Biology Laboratory, Biomedicine Discovery Institute, Monash University, Melbourne 3800, Australia; [b]Department of Anatomy and Developmental Biology, Monash University, Melbourne 3800, Australia; [c]Department of Obstetrics and Gynaecology, University of Melbourne, Royal Women's Hospital, Parkville, Victoria 3052, Australia; and [d]Bioinformatics, The Walter and Eliza Hall Institute of Medical Research, Parkville 3052, Australia

Edited by George E. Seidel, Colorado State University, Fort Collins, CO, and approved April 1, 2020 (received for review January 19, 2020)

Female fertility and offspring health are critically dependent on an adequate supply of high-quality oocytes, the majority of which are maintained in the ovaries in a unique state of meiotic prophase arrest. While mechanisms of DNA repair during meiotic recombination are well characterized, the same is not true for prophase-arrested oocytes. Here we show that prophase-arrested oocytes rapidly respond to γ-irradiation–induced DNA double-strand breaks by activating Ataxia Telangiectasia Mutated, phosphorylating histone H2AX, and localizing RAD51 to the sites of DNA damage. Despite mobilizing the DNA repair response, even very low levels of DNA damage result in the apoptosis of prophase-arrested oocytes. However, we show that, when apoptosis is inhibited, severe DNA damage is corrected via homologous recombination repair. The repair is sufficient to support fertility and maintain health and genetic fidelity in offspring. Thus, despite the preferential induction of apoptosis following exogenously induced genotoxic stress, prophase-arrested oocytes are highly capable of functionally efficient DNA repair. These data implicate DNA repair as a key quality control mechanism in the female germ line and a critical determinant of fertility and genetic integrity.

DNA repair | oocytes | fertility | apoptosis | DNA damage

Mammalian females are born with a stockpile of immature oocytes, which are housed in the ovary in structures called primordial follicles (1). These oocytes are maintained in a unique state of growth and meiotic prophase arrest for weeks, months, or even years before being activated to begin the developmental program that results in the ovulation of a fully mature oocyte that can support the development of healthy offspring. Primordial follicles cannot be replaced, even if the stockpile becomes prematurely exhausted, and their depletion results in infertility and loss of ovarian endocrine function. These characteristics make nongrowing prophase-arrested oocytes among the longest living cells in the female body and potentially vulnerable to DNA damage. It is imperative that their number, health, and genetic integrity are preserved throughout reproductive life to ensure fertility and perpetuation of the species.

Cells are subject to a range of exogenous and endogenous stressors that can lead to DNA damage. Among the many types of DNA damage, double-strand breaks (DSBs) are the most deleterious, promoting chromosome rearrangements and mutations. Moreover, DSBs can lead to genome instability if the breaks are repaired incorrectly or cause cell death if repair cannot be achieved. Like somatic cells, DNA DSBs can be generated in prophase-arrested oocytes following exposure to ionizing radiation, chemotherapeutic drugs, and environmental toxicants (2–4). DSBs may also accumulate in prophase-arrested oocytes over their prolonged life span as a consequence of normal metabolism, oxidative stress, and maternal aging (5). It would seem particularly important for prophase-arrested oocytes to correct this damage to their DNA so that sufficient numbers are retained in the ovary to ensure optimal fertility for an adequate period of time and to prevent the transmission of genetic defects to the next generation.

Immediately prior to prophase arrest, oocytes undergo meiotic recombination. During meiotic recombination, oocytes sustain hundreds of DSBs induced by Spo11, which are tolerated and subsequently repaired by homologous recombination (HR) (6). In stark contrast, however, the prophase-arrested oocytes in primordial follicles have an extremely low tolerance for DNA damage and readily undergo apoptosis when exposed to genotoxic stressors that somatic cells survive (2–4, 7, 8). Indeed, it has been proposed that the apoptotic elimination of damaged prophase-arrested oocytes is an essential mechanism for safeguarding the germ line from genetic defects and that the threshold for the cell death response in oocytes can be triggered by one irreparable DNA break (9). However, whether this sensitivity is because prophase-arrested oocytes have a uniquely low threshold for the activation of apoptosis, or are incapable of efficient error-free DNA repair, as previously implied, is not clear.

This study aimed to determine if prophase-arrested oocytes are capable of DSB repair and to provide insight into the role that DNA repair plays in determining the number and quality of oocytes available to support female reproduction. Using wild-type (WT) and apoptosis-deficient mice, we show that the nongrowing prophase-arrested oocytes residing in primordial follicles are capable of highly efficient DNA repair following exogenously induced DNA damage. We provide evidence to

Significance

An adequate supply of healthy oocytes is essential for female fertility. Oocytes that sustain even very low levels of DNA damage are killed, presumably because the damage is irreparable. Surprisingly, however, we show that when apoptosis is inhibited, oocytes can repair severe DNA damage via homologous recombination repair. The repair is highly efficient; it protects fertility and ensures the health and genetic integrity of offspring. These data implicate DNA repair as an additional quality control mechanism available within the female germ line.

Author contributions: J.M.S., M.W., and K.H. designed research; J.M.S., A.W., N.Z., M.W., and K.H. performed research; J.M.S., A.W., M.W., and K.H. analyzed data; and J.M.S., M.W., and K.H. wrote the paper.

The authors declare no competing interest.

This article is a PNAS Direct Submission.

Data deposition: Sequence data have been deposited in the National Center for Biotechnology Information Sequence Read Archive (accession no. PRJNA622592).

[1]To whom correspondence may be addressed. Email: karla.hutt@monash.edu.

This article contains supporting information online at https://www.pnas.org/lookup/suppl/doi:10.1073/pnas.2001124117/-/DCSupplemental.

First published May 7, 2020.

indicate that HR is the pathway used for DNA DSB repair and that this pathway effectively restores genetic integrity in oocytes. The outcomes of this study have important implications for our understanding of how the length of the fertile life span is regulated, the age at which menopause begins, and the mechanisms available within the female germ line to ensure transmission of high-fidelity genetic information to future generations. These findings may also be exploited to improve oocyte number and quality in women as they age and to develop new fertility preservation strategies for women exposed to DNA-damaging agents such as environmental toxicants and cancer treatments.

Materials and Methods

Animals. C57BL/6 and *TAp63*$^{-/-}$ (10) mice were housed under high-barrier conditions with a 12-h light–dark cycle and food and water ad libitum. All experiments were compliant with the National Health and Medical Research Council (NHMRC) Australian Code of Practice for the Care and Use of Animals and the Monash Animal Research Platform Animal Ethics Committee. Animals were time-mated, 10-d-old females were irradiated at 0.1, 0.2, 0.45, 4.5, or 7 Gy in a Gammacell40 Exactor Irradiator, and ovaries were collected 30 min, 3, 6, 24 h or 5 d after γ-irradiation. Ovaries were fixed in Bouins' solution or formalin, and tissue sections were prepared for stereology or immunofluorescent staining as described (11).

Follicle Enumeration. Follicle numbers were estimated using the optical fractionator stereological method or by performing direct counts as previously described (11, 12).

Immunofluorescence. DNA damage and repair markers were evaluated in prophase-arrested nongrowing (primordial follicles) and prophase-arrested growing (growing follicles) oocytes in three to six sections from formalin-fixed, paraffin-embedded, serially sectioned ovaries (n = 3 to 8 animals) as previously described (11). The primary antibodies used in this study were the following: 1/500 Ataxia Telangiectasia Mutated (ATM) (pS1981) antibody (BD Biosciences, 560007), 1/500 RAD51 (EPR4030) (3) antibody (Novus Biologicals, NBP1-95892), 1/500 anti–DNA-PKcs (phospho S2056) antibody (Abcam, ab18192), 1/200 Cleaved Caspase-3 (Asp175) (Cell Signaling Technology, 9661) and 1/500 phospho-histone γH2A.X (Ser139) (Cell Signaling Technology, 9718) paired with 1/500 CD117/c-kit antibody (R&D Systems, AF1356) to mark oocytes. Various combinations of ThermoFisher Scientific secondary donkey anti-mouse, anti-rabbit, and anti-goat antibodies conjugated to Alexa Fluor 488, 568, and 647 (A-11055, A-21202, A-21206, A-10042, A10037, A-31573, A-31571, and A-21447; ThermoFisher Scientific) were used at 1/500. For apoptosis assessment, one section on each slide was stained using Click-iT TUNEL FluorTM 647 Kit (ThermoFisher Scientific, C10247) as previously described (Stringer). Sections treated with DNase I were used as positive controls. Slides were cover-slipped with ProLong Diamond Antifade Mountant with DAPI (ThermoFisher Scientific, P36931) and imaged via a confocal Nikon C1 Upright 90i or Invert Ti-Ebase microscopes using the 40× oil objective with lasers of 405, 488, 561, and 638 nm (Nikon). Images were processed and analyzed using FIJI software (13).

Histopathology of Offspring from Irradiated Dams. Histopathology was undertaken by the Australian Phenomics Network, Histopathology and Organ Pathology Service, and examined by a qualified and experienced pathologist. The organs examined were the following: adrenal glands, bladder, bone marrow, brain, cecum, cervix, clitoral gland, colon, duodenum, epididymis, eyes, gall bladder, harderian glands, head, heart, hind leg (long bone, bone marrow, synovial joint, skeletal muscle), ileum, jejunum, kidney, liver, lungs, mammary tissue, mesenteric lymph node, ovaries, oviduct, pancreas, penis, preputial gland, prostate glands, salivary glands, regional lymph nodes, seminal vesicles, skin, spinal cord, stomach, tail, testes, thymus, thyroids, trachea, uterus, and vagina.

Oocyte and Embryo Collection. For superovulation, adult female mice were injected subcutaneously with 10 IU equine chorionic gonadotropin, followed 44 to 48 h later with 10 IU human chorionic gonadotropin. Oocytes were harvested from oviducts 12 to 14 h later, fixed for 15 min in 4% paraformaldehyde (PFA), and then stained with tubulin alpha, γH2A.X, and F-actin. For embryo collection, females were time-mated, and embryos were collected from plugged females on the day of plugging (embryonic day 0.5 [E0.5]) or 3 d post mating (E3.5), and embryos were flushed from the oviduct or uterus, respectively, and fixed for 15 min in 4% PFA at room temperature. Staining was performed in a 36-well plate transferring embryos and oocytes through a series of washes. All washes were performed in a 0.1% bovine serum albumin (BSA)/phosphate-buffered saline (PBS) + 1/1,000 Tween-20 + 1/10,000 Triton X-100 in PBS. Embryos and oocytes were first permeabilized in 1% Triton X-100 solution, washed, and then blocked for 1 h in 10% donkey serum in 3% BSA/PBS. Oocytes or embryos were incubated in primary antibodies for 1 h in PBS with 0.1% BSA in the following dilutions; 1/100 anti–β-tubulin (Sigma-Aldrich, T4026) and 1/1,000 phospho-histone γH2A.X (Ser139) (Cell Signaling Technology, 9718) or recombinant anti-CDX2 antibody (EPR2764Y) (Abcam, ab76541). Embryos and oocytes were washed before incubating in donkey anti-mouse 488 (Invitrogen, A-21202) and anti-rabbit 647 (Invitrogen, A-31573) secondary antibodies and F-actin 568 (Invitrogen, A-12374) stain for 1 h before washing and staining with 1:5,000 Hoechst 33342 (Thermo Scientific, 62249). Imaging of oocytes and embryos was performed using Leica SP8 Invert microscope, and images were processed and analyzed using FIJI software (13).

Fertility Studies. For assessment of fertility, adult female mice (untreated controls and γ-irradiated) were individually housed with untreated C57BL/6 males for 6 mo. Males were replaced if females were not pregnant within 1 mo, and females were plug-checked for 1 wk or until a plug was found after the addition of a new male.

Dual-Energy X-Ray Absorptiometry. Percentage fat, bone mineral content (BMC), and bone mineral density (BMD) were monitored by whole-body dual energy X-ray absorptiometry (DEXA) (Lunar PIXImus). Calibration was performed using a Quality Control Phantom before each run. All data were collected using Lunar PIXImus 2.0 software.

Whole-Genome Sequencing. Whole-genome sequencing (WGS) of 150-bp paired-end reads was conducted by Australian Genome Research Facility on the Illumina NovaSeq 6000 platform using the TruSeq DNA PCR-free all-inclusive WGS library protocol. As no offspring are produced from irradiated wild-type controls, we utilized two unirradiated *Tap63*$^{-/-}$ controls and a test population of 18 offspring from 0.45-Gy–treated females. Samples were sequenced to an average depth of 50-Gb genome coverage. To identify mutations characteristic of gamma-irradiation–induced DNA damage, we restricted our analysis to identifying haploid mutations that occurred in only one individual and did not overlap annotated mouse single-nucleotide polymorphisms (SNPs) or repeats. Reads were mapped to the GRCm38 genome with Bwa mem 0.7.15 (14), and individual samples were called for mutations with Octopus 0.5.2 (15). Unique mutations were identified and overlapped with SNPs and repeats with Bedtools 2.28 (16). Regions with candidate mutations were then recalled across the entire cohort with Platypus 0.8.1 (17) using population-based calling and manually inspected for local coverage, PCR duplicates, and flanking allelic bias. Sequences were uploaded to the National Center for Biotechnology Information Sequence Read Archive under accession no. PRJNA622592.

Treatment of TAp63$^{-/-}$ Mice with DNA-PKcs (NU7441) and Rad51 (B02) Inhibitors. Postnatal day (PN) 10 *TAp63*$^{-/-}$ mice were divided into four groups (n = 4/group) and treated (intraperitoneally) with the following: 1) 10 mg/kg DNA-PK inhibitor (NU7441, Tocris, 3712) in 4% dimethylsulfoxide (DMSO)/40% polyethylene glycol (PEG) 400/saline; 2) 50 mg/kg Rad51 inhibitor (B02, Merck, 553514) in 4% DMSO/40% PEG 400/saline; 3) NU7441(10 mg/kg) and B02 (50 mg/kg) combined in 4% DMSO/40% PEG 400/saline;, or 4) vehicle (4% DMSO/40% PEG 400/saline). Mice were γ-irradiated at 0.45 Gy within 1 h of injection, and ovaries were collected for analysis 24 h later.

Analysis and Statistics. Data are presented as means ± SEM. Statistical analyses were performed using GraphPad Prism software (GraphPad Software) and analyzed by one-way ANOVA, and the significance was determined by Tukey's post hoc multiple comparison test or Kruskal–Wallis for nonparametric data or by t tests for pairwise comparisons. Differences were considered significant when $P < 0.05$.

Data Availability. All sequence data are available at the National Center for Biotechnology Information Sequence Read Archive, and all other data are included in the paper and *SI Appendix*.

Results

Prophase-Arrested Oocytes Activate a DNA Repair Response. We first evaluated the DNA damage and repair response of oocytes by

exposing wild-type mice to increasing doses of whole-body γ-irradiation (0.2, 0.45, and 7 Gy) and monitoring the nuclear localization of phosphorylated ATM (pATM), a global regulator of the DNA damage response (Fig. 1*A*). For these studies, nongrowing prophase-arrested oocytes were classified as primordial follicles, whereas prophase-arrested oocytes that had initiated growth were classified as growing follicles.

While pATM was rarely detected in primordial follicles in untreated control mice, nuclear pATM was present in oocytes after γ-irradiation in a dose- and time-dependent manner (Fig. 1*A*). Initiation of the DNA damage response was accelerated at higher doses of γ-irradiation; 2.5% of primordial follicles were positive for pATM 0.5 h after 0.2 Gy, whereas 92% of oocytes were positive for pATM at 7 Gy. Furthermore, pATM localization was transient at 0.2 Gy, with the percentage of positive oocytes returning to basal levels at 6 h, but the response was sustained over this time frame at 7 Gy. pATM was also detected in the oocytes found in growing follicles after γ-irradiation, but to a lesser extent at the lowest dose of 0.2 Gy, suggesting that the DNA damage response may be more sensitive in primordial follicles (Fig. 1*A*).

The induction of DNA DSBs leads to the phosphorylation of histone H2AX on ser139 (γH2AX) by ATM kinase (18, 19). This results in the formation of discrete foci in a 1:1 ratio at the sites of DNA damage that facilitate the recruitment and targeting of repair factors. Thus, we next evaluated the formation of γH2AX foci at the sites of DNA damage (Fig. 1*B*). As expected, γH2AX foci were rarely observed in oocytes from untreated animals. However, γH2AX localized as discrete foci in oocytes within 0.5 h of γ-irradiation at all doses. Notably, the number of foci and the intensity of staining increased in a dose-dependent manner, indicative of increasing numbers of DNA DSBs (Fig. 1*C*). The oocytes in growing follicles exhibited a similar pattern of staining (Fig. 1*B*). Interestingly, γH2AX foci were less frequently observed in somatic cells than oocytes at the lowest dose of 0.2 Gy, suggesting that the DNA damage response may differ in sensitivity between germ cells and somatic cell lineages, with germ cells being more sensitive.

There are two main pathways responsible for repairing DNA DSBs, nonhomologous end joining (NHEJ) and HR (20). NHEJ can be undertaken at any stage of the cell cycle, is considered to be error prone (can leave insertions and deletions at the breakpoint), and is the predominant pathway employed by somatic cells (21). In contrast, HR results in accurate DNA repair but requires a template, and so its utility is largely restricted to the S-phase of the cell cycle (21). While well studied in somatic cells and oocytes undergoing meiotic recombination, very little is known about pathway choice in prophase-arrested oocytes. In order to gain insight into whether prophase-arrested oocytes can initiate a DNA repair response and whether HR and/or NHEJ pathways are utilized, we used RAD51 as a marker for HR and DNA-dependent protein kinase catalytic subunit (DNA-PKcs) as a marker for NHEJ. We found that RAD51 was localized to the sites of DNA damage in over 90% of oocytes in primordial follicles within 0.5 h of a 0.2- or 0.45-Gy exposure, whereas DNA-PKcs was detected in only ∼10% of primordial follicle oocytes, suggesting that HR is preferentially used (Fig. 1*D*). Prophase-arrested oocytes have replicated their DNA but have not yet undergone meiotic division and so have a repair template readily available to facilitate HR repair. Thus, our finding that the majority of prophase-arrested oocytes were positive for RAD51 is consistent with their cell-cycle status and with the use of HR machinery to repair DSBs induced by Spo11 during meiotic recombination (22). Conversely, granulosa cells were primarily positive for DNA-PKcs, with few RAD51 visible, although foci were not quantified in somatic cell populations, and so assessments remain qualitative (Fig. 1 *D* and *E*). Interestingly, at the higher dose of 7 Gy, the formation of RAD51 foci was slower, and the proportion of primordial follicle oocytes with RAD51 foci did not exceed 50% despite a rapid and strong pATM response and the detection of H2AX foci in most oocytes. Similar patterns of RAD51 and DNA-PKcs staining were observed in the oocytes of growing follicles.

Overall, these studies suggested that nongrowing and growing prophase-arrested oocytes are capable of initiating a DNA repair response and that HR is the predominant pathway. However, when we examined ovaries 24 h after γ-irradiation, we noted the presence of dying primordial follicles and that few healthy primordial follicles remained, even at a low 0.1-Gy dose (Fig. 1*F* and *SI Appendix*, Fig. S1). Strikingly, growing follicle numbers were largely unaffected and somatic cells remained intact, highlighting the unique sensitivity of nongrowing prophase-arrested oocytes in primordial follicles. As >90% of gametes found in the ovary are nongrowing prophase-arrested oocytes in primordial follicles, we focused on this stage of development for the rest of our studies.

Prophase-Arrested Oocytes Can Repair DNA DSBs When Apoptosis Is Inhibited. Having established that nongrowing prophase-arrested oocytes in primordial follicles can indeed initiate a DNA repair response, but nevertheless die, we wondered if this was due to a failure to complete repair efficiently. To begin to address this question, we took advantage of *TAp63*$^{-/-}$ mice. Previous studies have demonstrated that apoptosis in prophase-arrested oocytes in response to genotoxic stress is mediated by TAp63 and the transcriptional induction of the proapoptotic protein PUMA (2, 9). We first confirmed that oocytes in *TAp63*$^{-/-}$ mice survive doses of γ-irradiation lethal to oocytes in wild-type animals. *TAp63*$^{-/-}$ mice were untreated (controls) or exposed to 0.1, 0.45, or 7 Gy of whole-body γ-irradiation, and primordial follicles were enumerated 24 h later. In stark contrast to the significant depletion observed in wild-type mice (Fig. 1*F*), primordial follicle numbers in *TAp63*$^{-/-}$ mice following 0.1 and 0.45 Gy of γ-irradiation were similar to controls, although significant depletion was observed at the highest dose of 7 Gy (Fig. 2*A*).

We next used the formation and resolution of γH2AX foci to monitor the induction of DNA damage and subsequent repair in *TAp63*$^{-/-}$ mice (Fig. 2*B*). In *TAp63*$^{-/-}$ mice exposed to 0.1 Gy, ∼70% of oocytes were positive for γH2AX at 3 h, but this reduced to ∼40% by 24 h. At the higher dose of 0.45 Gy, 97% of oocytes were positive for γH2AX at 3 h and only 54% were positive at 24 h. Oocytes were largely devoid of γH2AX foci 5 d after γ-irradiation. Not only was the higher dose of 0.45 Gy associated with a higher percentage of oocytes positively labeled with γH2AX, but also the number of foci present indicated that the extent of DNA damage was more severe. The reduction in γH2AX foci suggests that many oocytes undertake repair within 24 h, with γH2AX-labeled lesions resolved within 5 d. Consistent with these findings, RAD51 followed a very similar staining pattern to that observed for γH2AX (Fig. 2*C*). Similar to our results in wild-type mice, at the higher 0.45-Gy dose, RAD51 foci were detected in 90% of oocytes at the 3-h time point, whereas DNA-PKcs was detected in only 10% of oocytes (Fig. 2 *C* and *D*), supporting the hypothesis that HR is the preferentially used pathway, although some oocytes may also undertake NHEJ.

To determine if RAD51 or DNA-PKcs are functionally important for DNA damage repair in prophase-arrested oocytes, we treated γ-irradiated (0.45 Gy) *TAp63*$^{-/-}$ mice with inhibitors of these proteins and evaluated oocyte survival. Notably, we found that the inhibition of RAD51, but not of DNA-PKcs, sensitized *TAp63*$^{-/-}$ prophase-arrested oocytes to γ-irradiation, indicated by the depletion of primordial follicle numbers, increased apoptosis of oocytes, and the persistence of unrepaired DSBs in those oocytes that survive (Fig. 2*E*). These observations support the conclusion that prophase-arrested oocytes rely on HR for the repair of DNA DSBs.

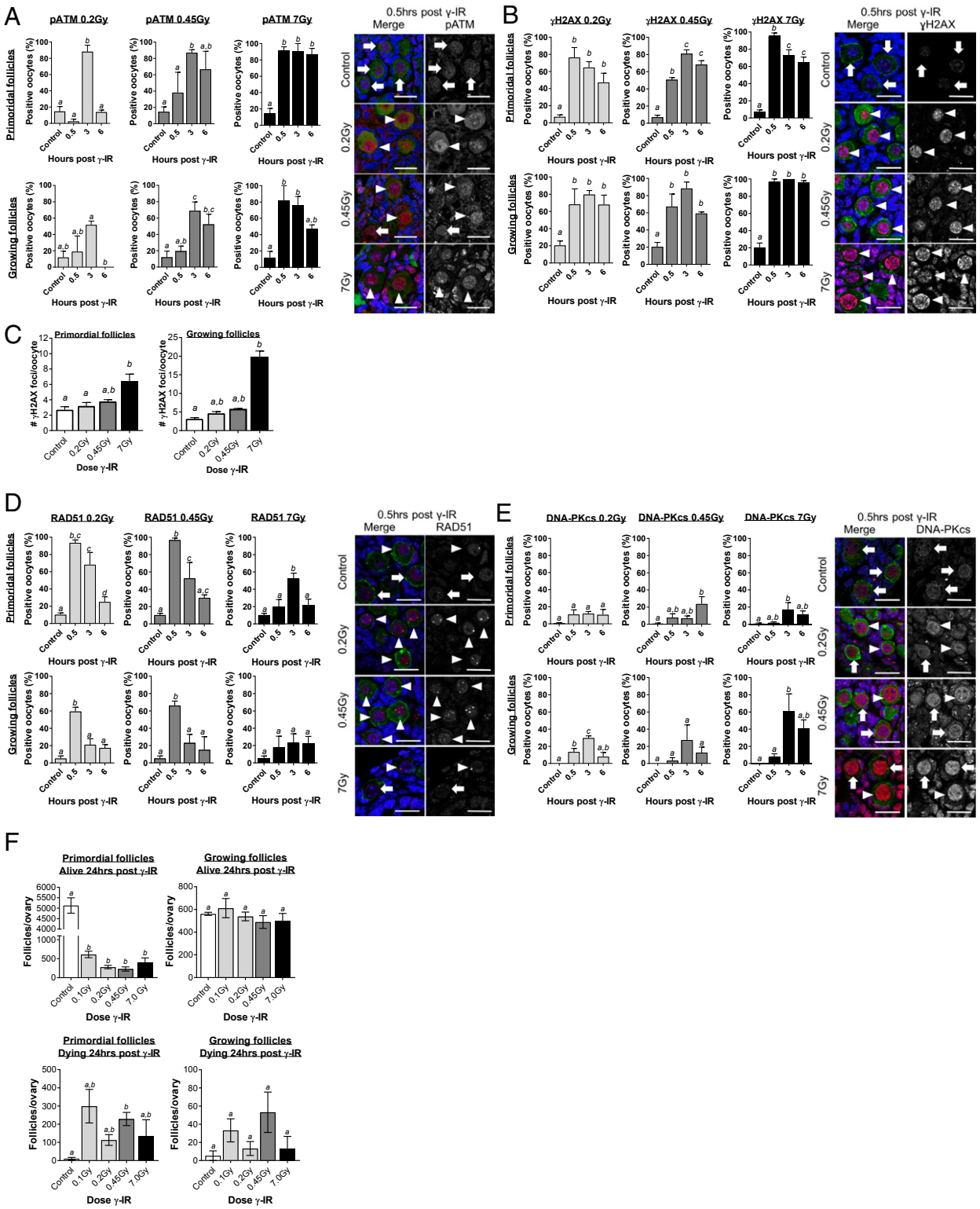

Fig. 1. The DNA repair response is activated in prophase-arrested oocytes following DNA damage. WT mice (PN10) were exposed to whole-body γ-irradiation at 0.2, 4.5, or 7 Gy. Prophase-arrested oocytes in primordial and growing follicles were analyzed in untreated controls 0.5, 3, and 6 h later for nuclear localization of pATM (*A*), γH2AX (*B* and *C*), RAD51 (*D*), and DNA-PKcs (*E*). Representative immunofluorescence images are shown for controls and at 0.5 h post γ-irradiation. DNA was counterstained with DAPI (blue), and oocytes were labeled with c-Kit or MVH (green) and colocalized with markers of the DNA damage response and repair (red; arrowheads indicate oocytes with positive staining, and arrows indicate negative staining) (Scale bars, 20 μm.) (*F*) Ovaries were also collected 24 h after γ-irradiation, and oocytes were enumerated ($n = 4$ to 5 mice/group). All data are expressed as mean ± SEM and analyzed by one-way ANOVA followed by Tukey's post hoc test or Kruskal–Wallis for nonparametric data. Different letters are significantly different; $P < 0.05$. Localization of each marker was evaluated in oocytes from ∼50 to 200 primordial follicles and ∼25 to 100 growing follicles per treatment and time point; $n = 3$–8 animals/group.

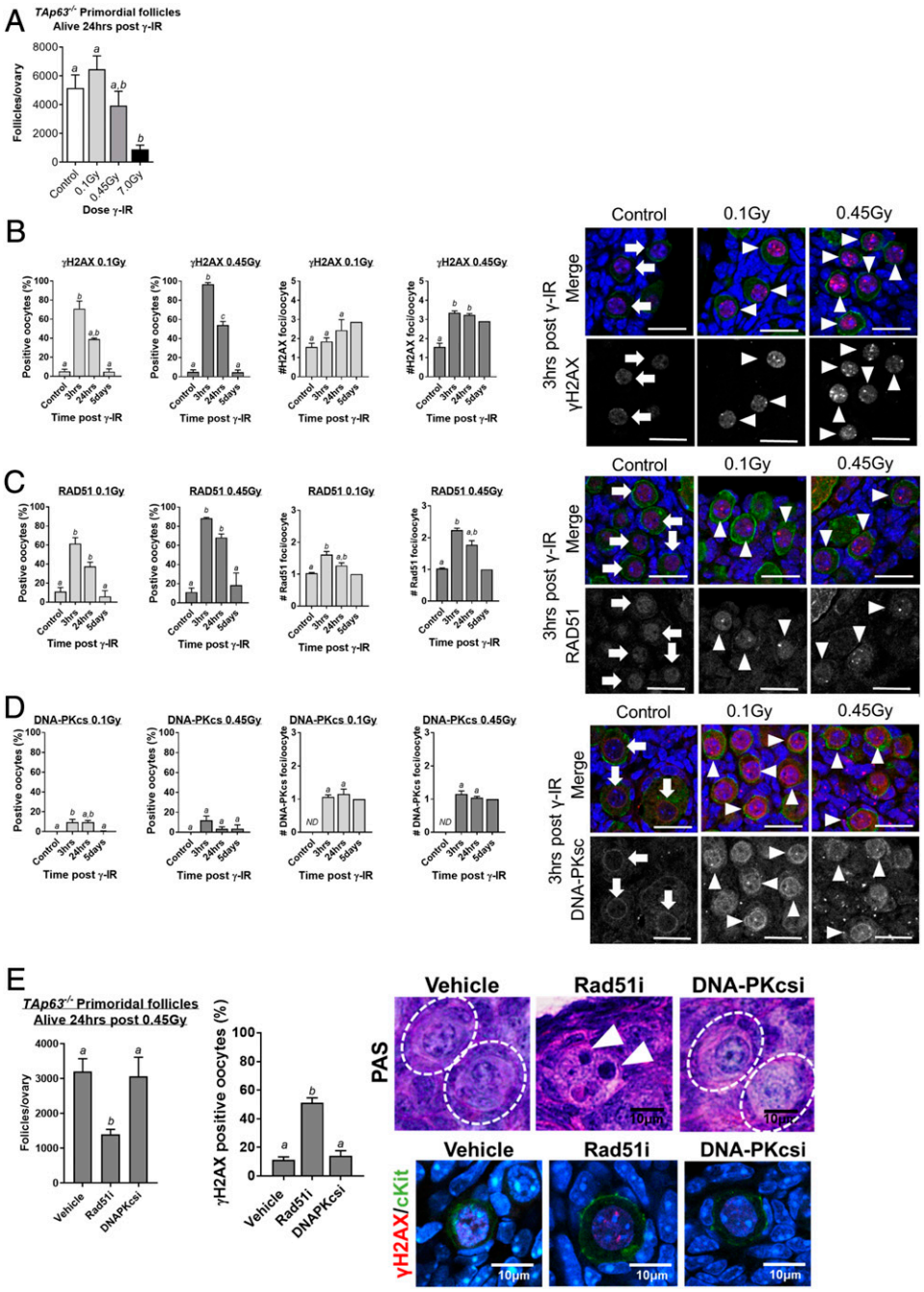

Fig. 2. Prophase-arrested oocytes can repair DNA when apoptosis is inhibited. (*A*) The number of primordial follicles in ovaries collected from *TAp63*$^{-/-}$ mice 24 h after γ-irradiation at 0.1, 0.45, and 7 Gy or from untreated control mice ($n = 3$ to 4 mice/group). The percentage of oocytes with γH2AX (*B*), RAD51 (*C*), and DNA-PKcs (*D*) foci and the average number of foci/oocyte in primordial follicles from control mice and *TAp63*$^{-/-}$ mice 3 h, 24 h, and 5 d after γ-irradiation at 0.1 Gy and 0.45 Gy. Localization of each marker was evaluated in ∼100 to 500 primordial follicle oocytes per treatment and time point; $n = 3$ to 8 animals/group. (*E*) γ-Irradiated (0.45 Gy) *TAp63*$^{-/-}$ mice were treated with vehicle, RAD51 inhibitor (Rad51i; 50 mg/kg, B02), or DNA-PK inhibitor (DNAPKcsi; 10 mg/kg, NU7441), and follicles were enumerated 24 h later ($n = 4$/group). Primordial follicles in vehicle and DNA-PKcs inhibitor-treated ovaries were of normal histological appearance (indicated by dashed-line white circles in PAS images), but apoptotic oocytes were observed in ovaries treated with the RAD51 inhibitor (indicated by white arrowheads in PAS images). The percentage of primordial follicle oocytes with γH2AX foci was calculated for each treatment group. All data are expressed as mean ± SEM and analyzed by one-way ANOVA followed by Tukey's post hoc test or Kruskal–Wallis for nonparametric data. Different letters are significantly different; $P < 0.05$. Absence of error bars in #H2AX foci/oocyte day 5 graphs (*B–D*) indicates too few oocytes with foci for statistical analysis.

DNA Repair Is Sufficient to Restore Functional Fertility. Our results indicate that 0.45 Gy is sufficient to induce approximately three DSBs in all of the prophase-arrested oocytes in primordial follicles from *TAp63*$^{-/-}$ mice (Fig. 2*B*). Our data also suggest that this DNA damage can be repaired when apoptosis is inhibited, at least to the extent of resolution of γH2AX foci (Fig. 2*B*, 5 d). Unrepaired or incorrectly repaired DSBs can result in chromosome breaks, translocations, deletions, and point mutations (23),

which could ultimately lead to oocyte apoptosis, impaired oocyte growth and maturation, infertility, miscarriage, or genetic defects in offspring (2, 24–26). To gain more insight into the quality and extent of repair, we investigated the ability of γ-irradiated prophase-arrested oocytes to subsequently develop to maturity, ovulate, and support normal embryonic development. WT and *TAp63*$^{-/-}$ mice were exposed to γ-irradiation at PN10, allowed to mature to adults, and then superovulated using exogenous hormonal stimulation. Although a small number of mature oocytes were obtained from WT mice exposed to 0.1 Gy, mature oocytes could not be harvested at the higher 0.45-Gy dose (Fig. 3*A*). Interestingly, large numbers of mature oocytes were ovulated in *TAp63*$^{-/-}$ mice exposed to 0.1 Gy, but only low numbers were obtained at the higher 0.45-Gy dose (Fig. 3*A*). It is not clear why this occurred, but may be due to a reduced ability of irradiated mice to respond to exogenous hormonal stimulation. Importantly, all harvested oocytes were at the meiotically mature Metaphase II (MII) stage and were morphologically normal with chromosomes aligned on the metaphase plate of the second meiotic spindle, a visible polar body, and absence of γH2AX foci (Fig. 3*A* and *SI Appendix*, Fig. S2).

We also assessed the number and morphology of zygotes and blastocysts derived from natural mating cycles (i.e., not hormonally stimulated) (Fig. 3 *B* and *C*). Normal numbers of zygotes were obtained from *TAp63*$^{-/-}$ mice exposed to 0.1 or 0.45 Gy, indicative of normal ovulation and fertilization rates. Furthermore, normal numbers of blastocysts developed in *TAp63*$^{-/-}$ mice exposed to 0.1 or 0.45 Gy, and total cell numbers and the ratio of inner cell mass to trophectoderm cells were normal, indicating normal preimplantation development. WT animals did not produce any zygotes or blastocysts, likely due to depletion of the primordial follicle pool.

We also assessed fertility by conducting a mating trial (Fig. 3*D*). We found that γ-irradiated *TAp63*$^{-/-}$ mice produced a similar number of litters as nonirradiated controls over the course of the study and that the litter size was comparable. As it is unlikely that oocytes with unrepaired DSBs could faithfully segregate chromosomes and chromatids to produce developmentally normal euploid embryos, these studies suggest that damaged oocytes have the capacity to sufficiently repair DNA damage to support oocyte development, meiotic maturation, preimplantation embryonic development, and fertility.

DNA Repair Is Sufficient to Maintain Offspring Health and Genetic Integrity. To further explore the ability of prophase-arrested oocytes to repair DNA damage, we extensively evaluated the health of offspring from γ-irradiated *TAp63*$^{-/-}$ dams (Fig. 4*A*). Offspring were well nourished, well groomed, and healthy with normal movement and gait. Offspring were weighed after birth (PN5), at weaning (PN19), and as young adults (PN65) (Fig. 4*B*). Weaning weights were slightly reduced in the male and female offspring from γ-irradiated dams compared to controls, possibly as a consequence of reduced maternal nutrition. This is suggested by the fact that the weights of adult female offspring from γ-irradiated dams were similar to controls, although they remained slightly lower in the male population. Further information about overall body composition was obtained in adult offspring from control and 0.45-Gy–exposed *TAp63*$^{-/-}$ dams using DEXA analyses; % fat, BMD, and BMC were comparable between groups and similar to values previously reported for C57BL/6 mice (27) (Fig. 4*D*). All offspring underwent autopsy, and major organs were inspected for gross morphology; no abnormalities were noted. The weights of the uterus, testis, hearts, kidneys, and livers were recorded, with slight weight changes noted for the liver and kidney (*SI Appendix*, Fig. S3). Ten untreated controls and 21 randomly selected offspring from 0.45-Gy–treated *TAp63*$^{-/-}$ dams also underwent complete histopathological analyses (50 organs), and no micromorphological changes or lesions of significance were identified. Overall, the number and percentage of offspring born to γ-irradiated dams that survived to sexual maturity were similar to controls (Fig. 4*C*), and female offspring were themselves fertile, a strong indicator of overall health (*SI Appendix*, Fig. S4).

Inaccurate DNA DSB repair can introduce random mutations, such as indels or point mutations. Therefore, in addition to phenotypic analyses in offspring, whole-genome sequencing was performed to identify mutations that could be attributed to radiation-induced damage. As no offspring were produced from irradiated WT mice, we utilized two offspring from unirradiated *TAp63*$^{-/-}$ dams as controls and a test population of 18 offspring from 0.45-Gy–treated *TAp63*$^{-/-}$ dams. A total of 15 (mean $5.2 \times 10^{-9} \pm 2.7 \times 10^{-9}$ per base per generation) and 32 mutations (mean $1.2 \times 10^{-9} \pm 0.44 \times 10^{-9}$ per base per generation) were identified in control and test groups, respectively (Fig. 4*D* and *SI Appendix*, Tables S1 and S2). Importantly, overall mutation rates did not increase in offspring from 0.45-Gy–treated *TAp63*$^{-/-}$ dams compared to control, consistent with the error-free repair of DNA DSBs in oocytes.

Discussion

Nongrowing prophase-arrested oocytes found in primordial follicles are the immature precursors of all ovulated oocytes. The apoptotic elimination of prophase-arrested oocytes with DNA damage is a well-characterized phenomenon and proposed to be a primary mechanism of quality control in the female germ line (28). Curiously, oocytes present in the developing fetus undergoing meiotic recombination tolerate hundreds of DNA DSBs, but a short time later, a single DSB is sufficient to trigger apoptosis of the prophase-arrested oocytes in primordial follicles (9). Because of their low threshold for the activation of apoptosis, it was not clear whether prophase-arrested oocytes could mount a functionally effective DNA repair response to correct damage.

This lack of clarity is also partly because previous studies utilizing genetic mouse models of DSB repair deficiency are confounded by the essential role of HR in the repair of meiotically programmed DSBs (5, 29). For example, reduced numbers of prophase-arrested oocytes (i.e., primordial follicles) were observed in adult BRCA1$^{+/\Delta 11}$ mice (5). While potentially supportive of a role for HR in the survival of prophase-arrested oocytes, this phenotype may also be attributed to the elimination of oocytes at meiotic recombination, and thus failure to establish adequate numbers of primordial follicles in the ovarian reserve around the time of birth. The few other studies that have investigated DNA repair function in female gametes in mice, cows, or humans have used fully grown (referred to as the germinal vesicle stage) or ovulated oocytes (5, 30–33), which exhibit vastly different characteristics to prophase-arrested oocytes in primordial follicles, including a heightened resistance to DNA damage (34). Thus, these earlier studies are unable to provide direct insight into the ability of nongrowing prophase-arrested oocytes to undertake DNA repair. We have addressed this fundamental knowledge gap by focusing on primordial follicles and now provide direct evidence to show that nongrowing prophase-arrested oocytes can repair exogenously induced DSBs, primarily using the HR repair pathway, and that this repair is sufficient to restore oocyte quality and support fertility without compromising offspring health or genetic integrity.

Additional support for our finding that prophase-arrested oocytes can repair exogenously induced DSBs comes from elegant studies revealing a role for CHK2 kinase in activating apoptosis in response to unresolved meiotic DSBs (35, 36). During meiosis, the repair of meiotically programmed DSBs into noncrossovers requires TRIP13. Oocytes die in *Trip13*$^{Gt/Gt}$ mice due to lack of timely DSB repair, but loss of CHK2 rescued a small cohort, and *Chk2*$^{-/-}$*Trip13*$^{Gt/Gt}$ mice were shown to be partially

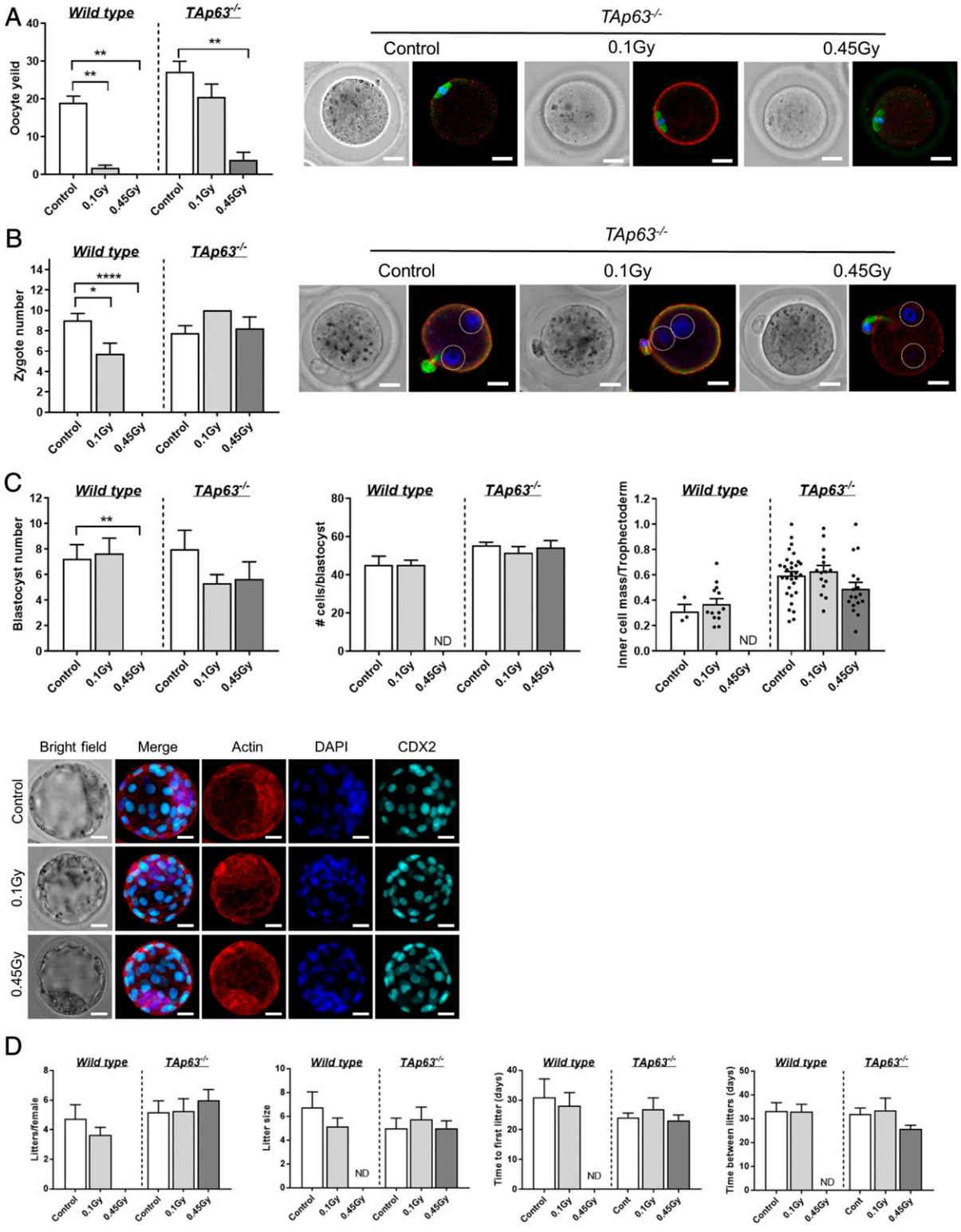

Fig. 3. DNA repair is sufficient to restore functional fertility. (*A*) Number of ovulated oocytes harvested from γ-irradiated wild-type and *TAp63*$^{-/-}$ mice following exogenous hormonal stimulation. Representative images of oocytes obtained from *TAp63*$^{-/-}$ females stained with f-actin (red) to mark the oolema, αβ-tubulin (green) to label the spindle, and DAPI to label the DNA on the metaphase plate. (*B*) Number of zygotes obtained from γ-irradiated WT and *TAp63*$^{-/-}$ mice at E0.5 after mating with untreated males. Representative images of zygotes obtained from *TAp63*$^{-/-}$ females stained with f-actin (red) to mark the zygote boundary and with DAPI to label the DNA in pronuclei (circled by dotted white lines) to confirm fertilization. (Scale bar, 20 μm.) (*C*) Number of blastocysts obtained from γ-irradiated WT and *TAp63*$^{-/-}$ mice at E3.5 after mating with untreated males. The ratio of inner cell mass to trophectoderm (TE) is shown. Representative images of blastocysts obtained from *TAp63*$^{-/-}$ females stained with f-actin (red) to mark the cell boundaries and with DAPI to label the DNA and CDX2 (aqua) to label TE. (Scale bar, 20 μm.) Fertility of mice (*D*) from continuous mating trial. All data are expressed as mean ± SEM and analyzed by one-way ANOVA followed by Tukey's post hoc test or Kruskal–Wallis for nonparametric data or *t* tests for pairwise comparisons. Different letters are significantly different; $*P < 0.05$, $**P < 0.005$, $****P < 0.0001$.

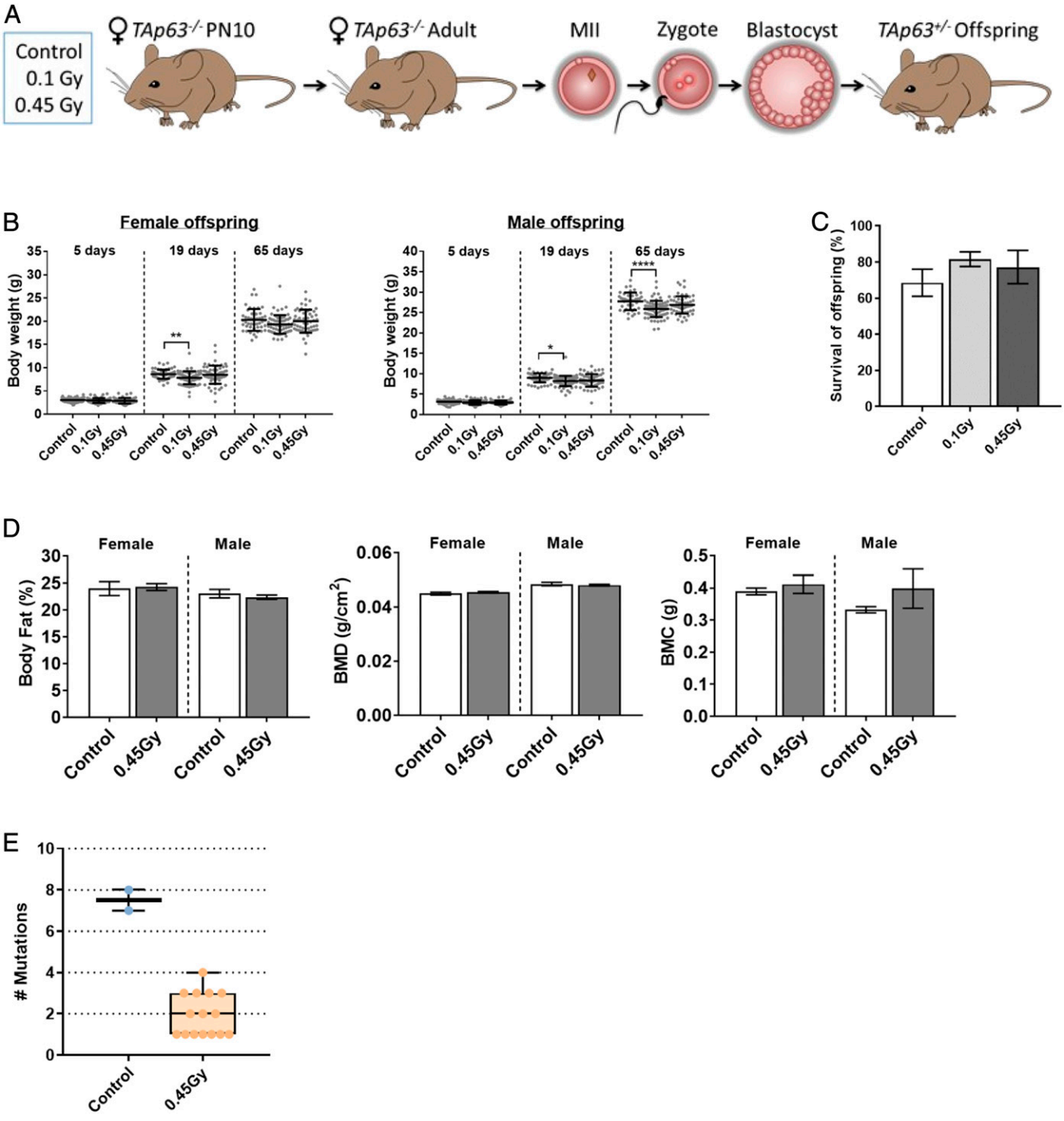

Fig. 4. Offspring from γ-irradiated *TAp63*$^{-/-}$ dams are healthy. (*A*) *TAp63*$^{-/-}$ mice were untreated or γ-irradiated at PN10. Adults were then mated with untreated WT males, and offspring health analyzed. (*B*) Weight of female and male offspring from control, 0.1 Gy, and 0.45 Gy *TAp63*$^{-/-}$ dams at 5, 19, and 65 d after birth. Dots represent weights for individual animals. Female/male n = 62/55, 62/74, 64/65 for control, 0.1 Gy, and 0.45 Gy. (*C*) Percentage of offspring from control, 0.1 Gy, and 0.45 Gy *TAp63*$^{-/-}$ dams that survive to 65 d (adulthood). (*D*) Percentage of fat, bone mineral density, and bone mineral composition were determined by DEXA in male and female offspring from control and 0.45-Gy *TAp63*$^{-/-}$ dams at 65 d. Female/male n = 19/40, 51/110 for control and 0.45 Gy. Data for *B*–*D* are expressed as mean ± SEM and analyzed by one-way ANOVA followed by Tukey's post hoc test. *$P < 0.05$, **$P < 0.005$, ****$P < 0.0001$. No significant differences were observed in *B* and *C*. (*E*) The genomes of two offspring from unirradiated *TAp63*$^{-/-}$ control dams (n = 2) and 18 offspring from 0.45-Gy–treated *TAp63*$^{-/-}$ dams (n = 5) were sequenced. Box and whisker plots of mutations in the 1.4 Gbp assayed per animal are shown. *TAp63*$^{+/-}$ offspring from irradiated dams have a significantly lower mutation rate than controls ($1.2 \times 10^{-9} \pm 0.44 \times 10^{-9}$ vs. $5.2 \times 10^{-9} \pm 2.7 \times 10^{-9}$ $P = 4.2 \times 10^{-6}$ Poisson generalized linear model mutations ~ genotype).

fertile despite the persistence of meiotic DSB into prophase arrest. Although not experimentally explored in this earlier work, the fertility of $Chk2^{-/-}Trip13^{Gt/Gt}$ mice suggests that persistent meiotic DSBs caused by loss of TRIP13 activity were eventually repaired in the surviving oocytes sometime during their prophase arrest.

Uniquely, nongrowing prophase-arrested oocytes have undergone a round of DNA replication in the absence of cell division. Thus, a DNA template (e.g., sister chromatid) is available for accurate, error-free repair by HR. RAD51 is essential for HR repair in somatic cells and is among the few specific repair factors proven to be expressed in primordial follicle oocytes (31). In our study, the localization of RAD51 to sites of exogenously induced DSBs in ∼90% of irradiated prophase-arrested oocytes—combined with their significantly increased sensitivity to DNA damage when RAD51 was inhibited and the very low mutation rate in offspring derived from damaged oocytes—supports the hypothesis that the majority of prophase-arrested oocytes utilize the HR pathway. This pathway choice is different from that of somatic cells, in which some evidence suggests that NHEJ is the default mechanism for DSB repair, even in the G2 phase of the cell cycle when a sister chromatid is available for HR (37).

Although HR appears to predominate, some DSBs may be repaired by the more error-prone pathway of NEHJ, indicated by the presence of DNA-PKcs foci in 10% of prophase-arrested oocytes. Functionally, the importance of NHEJ for the maintenance of oocyte quality is unclear; female mice deficient in DNA-PKcs are fertile (38), but Ku70 and Ku80 mutants (key proteins in the NHEJ pathway) rarely produce offspring (39, 40), although the cause of their subfertility has not been investigated. The mechanisms underlying the choice between DSB repair pathways in mammalian cells are not fully understood and likely complex (20, 41). Why some oocytes might undertake NHEJ instead of HR requires further study.

Interestingly, we observed a lower mutation rate in offspring derived from 0.45-Gy–exposed dams than in offspring from unexposed dams. At present we cannot confirm why this occurs, but one possibility is that an inducible response is required to repair the low levels of DNA damage that occur naturally in oocytes. In other words, it is possible that the repair response triggered by radiation-induced DNA damage also results in the repair of endogenous damage that would normally be insufficient to activate repair processes. In support of this theory, studies in a variety of somatic cells have shown that very low levels of DNA damage can fail to elicit a repair response (i.e., the damage persists with the potential to introduce mutations), but repair of this damage can be stimulated when the DNA damage response is triggered by another insult (42). Our results suggest that this phenomenon should be investigated further in oocytes.

Our data using $TAp63^{-/-}$ mice highlight the possibility that apoptosis may not be an essential quality control mechanism in response to DNA damage within the female germ line and that DNA repair can restore oocyte quality and maintain oocyte number, thereby ensuring fertility and the health and genetic integrity of offspring. This work raises this intriguing question: If prophase-arrested oocytes can repair DNA efficiently, why do they so readily undergo apoptosis when exposed to exogenous DNA-damaging agents? Oocyte apoptosis has significant consequences, as it depletes the ovarian reserve of primordial follicles and reduces the fertile life span, or causes infertility if the depletion is severe (2, 7). This question remains unanswered, but one possibility is that the evolutionary purpose of TAp63, the most ancient member of the p53 family, is to induce apoptosis of oocytes that fail to successfully complete meiotic recombination, thereby serving as a "recombination checkpoint" (43). If this is the case, then the rapid induction of apoptosis by Tap63 in response to exogenously induced DNA damage may just be a secondary consequence of its primary role.

In addition to improving our understanding of the fundamental mechanisms underlying the regulation of oocyte number and quality, the findings reported here may be of relevance for women undergoing cancer treatments, a devastating side effect of which is DNA-damage–induced death of nongrowing prophase-arrested oocytes. Depletion of these oocytes commonly leads to infertility and early menopause in female cancer survivors. Blocking oocyte death is being actively investigated as one of the most promising methods to preserve future fertility and endocrine health in female cancer patients (44), but this strategy will be feasible only if oocytes can repair the damage they have sustained. Our work in mice provides direct evidence to support the hypothesis that oocytes do indeed have the capacity to repair DSBs and that this repair may be able to protect fertility and retain genetic fidelity of offspring. It is worth considering, however, that oocyte and follicle responses to DNA damage and the efficiency of DNA repair may be different in prepubertal mice (used in this study) when compared to young adults or during maternal aging. Thus, future work should address the possibility that DNA damage responses may vary with age.

ACKNOWLEDGMENTS. We thank from Monash Micro Imaging and the Monash Histology Platform for services and support. This work was supported by the National Health and Medical Research Council Grants 1050130 and 1100219 (to K.H.) and made possible through the Victorian State Government Operational Infrastructure Support and the Australian Government NHMRC Independent Research Institute Infrastructure Support Scheme.

1. J. K. Findlay, K. J. Hutt, M. Hickey, R. A. Anderson, How is the number of primordial follicles in the ovarian reserve established? *Biol. Reprod.* **93**, 111 (2015).
2. J. B. Kerr *et al*., DNA damage-induced primordial follicle oocyte apoptosis and loss of fertility require TAp63-mediated induction of Puma and Noxa. *Mol. Cell* **48**, 343–352 (2012).
3. J. B. Kerr *et al*., Cisplatin-induced primordial follicle oocyte killing and loss of fertility are not prevented by imatinib. *Nat. Med.* **18**, 1170–1172, author reply 1172–1174 (2012).
4. J. B. Kerr *et al*., The primordial follicle reserve is not renewed after chemical or γ-irradiation mediated depletion. *Reproduction* **143**, 469–476 (2012).
5. S. Titus *et al*., Impairment of BRCA1-related DNA double-strand break repair leads to ovarian aging in mice and humans. *Sci. Transl. Med.* **5**, 172ra21 (2013).
6. F. Baudat, Y. Imai, B. de Massy, Meiotic recombination in mammals: Localization and regulation. *Nat. Rev. Genet.* **14**, 794–806 (2013).
7. Q. N. Nguyen *et al*., Loss of PUMA protects the ovarian reserve during DNA-damaging chemotherapy and preserves fertility. *Cell Death Dis.* **9**, 618 (2018).
8. A. L. Winship, M. Bakai, U. Sarma, S. H. Liew, K. J. Hutt, Dacarbazine depletes the ovarian reserve in mice and depletion is enhanced with age. *Sci. Rep.* **8**, 6516 (2018).
9. E. K. Suh *et al*., p63 protects the female germ line during meiotic arrest. *Nature* **444**, 624–628 (2006).
10. X. Guo *et al*., TAp63 induces senescence and suppresses tumorigenesis in vivo. *Nat. Cell Biol.* **11**, 1451–1457 (2009).
11. J. M. Stringer, E. O. K. Swindells, N. Zerafa, S. H. Liew, K. J. Hutt, Multi-dose 5-Fluorouracil is highly toxic to growing ovarian follicles in mice. *Toxicol. Sci.* **166**, 97–107 (2018).
12. M. Myers, K. L. Britt, N. G. Wreford, F. J. Ebling, J. B. Kerr, Methods for quantifying follicular numbers within the mouse ovary. *Reproduction* **127**, 569–580 (2004).
13. J. Schindelin *et al*., Fiji: An open-source platform for biological-image analysis. *Nat. Methods* **9**, 676–682 (2012).
14. H. Li, Aligning sequence reads, clone sequences and assembly contigs with BWA-MEM. arxiv:1303.3997 (16 March 2013).
15. D. Cooke, D. Wedge, G. Lunter, A unified haplotype-based method for accurate and comprehensive variant calling. https://doi.org/10.1101/456103 (29 October 2018).
16. A. R. Quinlan, I. M. Hall, BEDTools: A flexible suite of utilities for comparing genomic features. *Bioinformatics* **26**, 841–842 (2010).
17. A. Rimmer *et al*.; WGS500 Consortium, Integrating mapping-, assembly- and haplotype-based approaches for calling variants in clinical sequencing applications. *Nat. Genet.* **46**, 912–918 (2014).
18. K. K. Khanna, M. F. Lavin, S. P. Jackson, T. D. Mulhern, ATM, a central controller of cellular responses to DNA damage. *Cell Death Differ.* **8**, 1052–1065 (2001).

19. S. K. Mahadevaiah *et al*., Recombinational DNA double-strand breaks in mice precede synapsis. *Nat. Genet.* **27**, 271–276 (2001).
20. R. Scully, A. Panday, R. Elango, N. A. Willis, DNA double-strand break repair-pathway choice in somatic mammalian cells. *Nat. Rev. Mol. Cell Biol.* **20**, 698–714 (2019).
21. Z. Mao, M. Bozzella, A. Seluanov, V. Gorbunova, DNA repair by nonhomologous end joining and homologous recombination during cell cycle in human cells. *Cell Cycle* **7**, 2902–2906 (2008).
22. N. Hunter, Meiotic recombination: The essence of heredity. *Cold Spring Harb. Perspect. Biol.* **7**, a016618 (2015).
23. S. E. Polo, S. P. Jackson, Dynamics of DNA damage response proteins at DNA breaks: A focus on protein modifications. *Genes Dev.* **25**, 409–433 (2011).
24. M. M. van den Berg, M. C. van Maarle, M. van Wely, M. Goddijn, Genetics of early miscarriage. *Biochim. Biophys. Acta* **1822**, 1951–1959 (2012).
25. K. Zou *et al*., Production of offspring from a germline stem cell line derived from neonatal ovaries. *Nat. Cell Biol.* **11**, 631–636 (2009).
26. L. G. Shaffer, J. R. Lupski, Molecular mechanisms for constitutional chromosomal rearrangements in humans. *Annu. Rev. Genet.* **34**, 297–329 (2000).
27. S. Gargiulo *et al*., Evaluation of growth patterns and body composition in C57Bl/6J mice using dual energy X-ray absorptiometry. *BioMed Res. Int.* **2014**, 253067 (2014).
28. A. J. Levine, R. Tomasini, F. D. McKeon, T. W. Mak, G. Melino, The p53 family: Guardians of maternal reproduction. *Nat. Rev. Mol. Cell Biol.* **12**, 259–265 (2011).
29. A. Inagaki, R. Roset, J. H. Petrini, Functions of the MRE11 complex in the development and maintenance of oocytes. *Chromosoma* **125**, 151–162 (2016).
30. L. L. Kujjo *et al*., RAD51 plays a crucial role in halting cell death program induced by ionizing radiation in bovine oocytes. *Biol. Reprod.* **86**, 76 (2012).
31. L. L. Kujjo *et al*., Enhancing survival of mouse oocytes following chemotherapy or aging by targeting Bax and Rad51. *PLoS One* **5**, e9204 (2010).
32. P. Marangos *et al*., DNA damage-induced metaphase I arrest is mediated by the spindle assembly checkpoint and maternal age. *Nat. Commun.* **6**, 8706 (2015).
33. J. K. Collins, S. I. R. Lane, J. A. Merriman, K. T. Jones, DNA damage induces a meiotic arrest in mouse oocytes mediated by the spindle assembly checkpoint. *Nat. Commun.* **6**, 8553 (2015).
34. P. Marangos, J. Carroll, Oocytes progress beyond prophase in the presence of DNA damage. *Curr. Biol.* **22**, 989–994 (2012).
35. E. Bolcun-Filas, V. D. Rinaldi, M. E. White, J. C. Schimenti, Reversal of female infertility by Chk2 ablation reveals the oocyte DNA damage checkpoint pathway. *Science* **343**, 533–536 (2014).
36. V. D. Rinaldi, E. Bolcun-Filas, H. Kogo, H. Kurahashi, J. C. Schimenti, The DNA damage checkpoint eliminates mouse oocytes with chromosome synapsis failure. *Mol. Cell* **67**, 1026–1036.e2 (2017).
37. J. Her, S. F. Bunting, How cells ensure correct repair of DNA double-strand breaks. *J. Biol. Chem.* **293**, 10502–10511 (2018).
38. A. Kurimasa *et al*., Catalytic subunit of DNA-dependent protein kinase: Impact on lymphocyte development and tumorigenesis. *Proc. Natl. Acad. Sci. U.S.A.* **96**, 1403–1408 (1999).
39. X. C. Li, J. C. Schimenti, Mouse pachytene checkpoint 2 (trip13) is required for completing meiotic recombination but not synapsis. *PLoS Genet.* **3**, e130 (2007).
40. Z. Li *et al*., Alteration in the GyrA subunit of DNA gyrase and the ParC subunit of DNA topoisomerase IV in quinolone-resistant clinical isolates of Staphylococcus epidermidis. *Antimicrob. Agents Chemother.* **42**, 3293–3295 (1998).
41. Y. Zhou *et al*., Regulation of the DNA damage response by DNA-PKcs inhibitory phosphorylation of ATM. *Mol. Cell* **65**, 91–104 (2017).
42. S. Grudzenski, A. Raths, S. Conrad, C. E. Rübe, M. Löbrich, Inducible response required for repair of low-dose radiation damage in human fibroblasts. *Proc. Natl. Acad. Sci. U.S.A.* **107**, 14205–14210 (2010).
43. J. Carroll, P. Marangos, The DNA damage response in mammalian oocytes. *Front. Genet.* **4**, 117 (2013).
44. Y. Luan, M. E. Edmonds, T. K. Woodruff, S. Y. Kim, Inhibitors of apoptosis protect the ovarian reserve from cyclophosphamide. *J. Endocrinol.* **240**, 243–256 (2019).